

EFFICIENT ELECTRICALLY SMALL PROLATE SPHEROIDAL ANTENNAS COATED WITH A SHELL OF DOUBLE-NEGATIVE METAMATERIALS

M. D. Huang and S. Y. Tan

School of Electrical and Electronic Engineering
Nanyang Technological University
50 Nanyang Avenue, 639798, Singapore

Abstract—An efficient, electrically small prolate spheroidal antenna coated with confocal double-negative (DNG) metamaterials (MTMs) shell is presented. The radiation power of this antenna-DNG shell system excited by a delta voltage across an infinitesimally narrow gap around the antenna center is obtained using the method of separation of the spheroidal scalar wave functions. Our results show that this electrically small dipole-DNG shell system has very high radiation efficiency comparing with the normal electrically small antenna due to the inductive effect of the MTMs shell that cancel with the capacitive effect of the electrically small antenna. It is found that the spheroidal shell can achieve more compact structure and higher radiated power ratio than the corresponding spherical shell. This dipole-DNG shell systems with different sizes are analyzed and discussed.

1. INTRODUCTION

In all areas of electrical engineering, there has been much interest in miniaturization of the electronic devices, such as in electromagnetics and antennas [1–6]. Electrically small antennas are antennas with small geometrical dimensions compared to the wavelength of the electromagnetic (EM) fields they radiate. More specifically, an electrically small antenna in free space is defined as $k_0 r_e \leq 0.5$ in [5] where k_0 is the wave number in free space and r_e is the effective radius of the sphere enclosed the electrically small antenna.

With the development of wireless technologies for communications and sensor network, the efficient, electrically small antennas with wide bandwidth are desirable. However, these requirements are always contradictory. It is well-known that electrically small dipole

antennas in free space are inefficient radiators because of having a very small resistance and very large capacitive reactance. However, with the development of new materials, such as MTMs, there is a new challenging opportunity to solve this limitation. MTMs are artificial constructed materials which are engineered media having qualitatively new response functions that do not occur or may not be easily available in nature [7], which have gained increasing interest [8–20]. Efficient electrically small antennas have been constructed by coating a DNG or epsilon-negative (ENG) MTMs shell [8, 9], which have both large overall efficiency and large FBW. This is based on the MTMs shell has inductive reactance from a circuit point of view, while the electrically small antenna has capacitive reactance. Therefore, the electrically small antenna and the DNG MTMs shell are matched to form a resonant CL circuit, and the radiated power is greatly enhanced.

Spheroidal wave functions are special functions in mathematical physics [21] which have many applications [22, 23], especially in the analysis and design of antennas [24–27], since spheroidal antennas can be used to model many antenna shapes, from wire/cylindrical antennas via spherical antennas to disk antennas. And the full-wave analyses of the spheroidal antennas coated with a confocal radome are presented in [26]. In this paper, an electrically small prolate spheroidal antenna coated with confocal DNG MTMs shell is investigated. DNG MTMs studied in this paper is assumed to be lossless and nondispersive. The excitation is assumed to be a delta voltage across an infinitesimally narrow gap around the antenna center. The solution of the radiation power is obtained using the method of separation of the spheroidal scalar wave functions. Our results show that this electrically small dipole-DNG shell system has very high radiation efficiency comparing with the normal electrically small antenna. It is found that the spheroidal shell can achieve more compact structure and higher radiated power ratio than the corresponding spherical shell. This dipole-DNG shell systems with different sizes are analyzed and discussed.

2. FORMULATIONS

2.1. Geometry of Prolate Spheroidal Antenna

A perfectly conducting prolate spheroidal antenna coated with a confocal spheroidal DNG MTMs shell, as shown in Fig. 1, is studied in this paper, which is assumed to be excited by a source field E^a over a infinitesimal gap on its surface center. In the prolate spheroidal coordinates (η, ξ, ϕ) , the surfaces from inner to outer spheroid are given by $\xi = \xi_1$, $\xi = \xi_2$, and $\xi = \xi_3$ respectively, the length of the

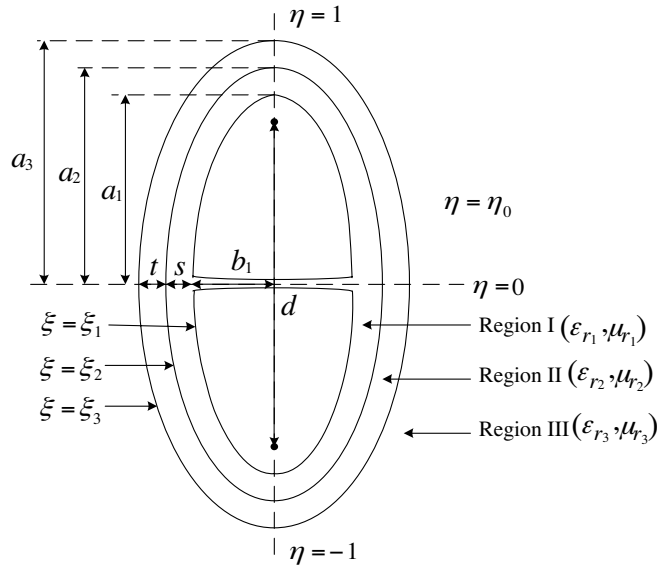


Figure 1. Geometry of the problem.

corresponding semimajor and semiminor axes are a_1 , a_2 , a_3 , and b_1 , b_2 , b_3 respectively, and the length of the common interfocal distance is d , which have the relation as follows,

$$\xi = \frac{2a}{d} = \frac{a}{\sqrt{a^2 - b^2}} \quad (1)$$

The thickness of the DNG MTMs shell layer along the semiminor axis is denoted as $t = b_3 - b_2$. The separation between the antenna and the shell is denoted as $s = b_2 - b_1$. The media of the coating layers in region I, II and III are all assumed to be linear, homogeneous, isotropic, lossless and nondispersive with relative permittivities ϵ_{r1} , ϵ_{r2} , and ϵ_{r3} and relative permeabilities μ_{r1} , μ_{r2} , and μ_{r3} respectively. The region I and III are usually free space with permittivity ϵ_0 and permeability μ_0 . A time dependence of $e^{j\omega t}$ is assumed and suppressed throughout.

2.2. Prolate Spheroidal Antenna Coated with a DNG MTMs Shell

Due to the symmetry (i.e., $\partial/\partial\phi = 0$), the Maxwell's equations in free space are as follows,

$$j\omega\epsilon_0 E_\xi = \frac{1}{h_\eta h_\phi} \frac{\partial(h_\phi H_\phi)}{\partial\eta} \quad (2a)$$

$$jw\epsilon_0 E_\eta = -\frac{1}{h_\phi h_\xi} \frac{\partial(h_\phi H_\phi)}{\partial \xi} \quad (2b)$$

$$jw\mu_0 H_\phi = \frac{1}{h_\xi h_\eta} \left[\frac{\partial(h_\xi E_\xi)}{\partial \eta} - \frac{\partial(h_\eta E_\eta)}{\partial \xi} \right] \quad (2c)$$

where the metrical coefficients h_η , h_ξ , and h_ϕ in prolate spheroidal coordinates are defined by

$$h_\eta = \frac{d}{2} \left(\frac{\xi^2 - \eta^2}{1 - \eta^2} \right)^{\frac{1}{2}} \quad (3a)$$

$$h_\xi = \frac{d}{2} \left(\frac{\xi^2 - \eta^2}{\xi^2 - 1} \right)^{\frac{1}{2}} \quad (3b)$$

$$h_\phi = \frac{d}{2} [(\xi^2 - 1)(1 - \eta^2)]^{\frac{1}{2}} \quad (3c)$$

It is seen from (2) that if the source field on the gap has only E_η component, the excited magnetic field will have only H_ϕ component and $E_\phi = 0$. It can be shown that the EM fields can be determined in terms of an auxiliary scalar wave function A [24],

$$H_\phi = \frac{A}{h_\phi} \quad (4)$$

$$E_\xi = \frac{4}{jw\epsilon_0 d^2} \frac{1}{\sqrt{(\xi^2 - 1)(\xi^2 - \eta^2)}} \frac{\partial A}{\partial \eta} \quad (5)$$

$$E_\eta = -\frac{4}{jw\epsilon_0 d^2} \frac{1}{\sqrt{(1 - \eta^2)(\xi^2 - \eta^2)}} \frac{\partial A}{\partial \xi} \quad (6)$$

The auxiliary wave function in region I ($\xi_1 \leq \xi \leq \xi_2$) can be expressed as follows [26],

$$A_1 = \sum_{n=1,2}^{\infty} V_n(h_1, \eta) \left[M_n^1 \left(U_n(h_1, \xi) - \frac{U'_n(h_1, \xi_1) T_n(h_1, \xi)'_n}{T} (h_1, \xi_1) \right) + \frac{p_n T_n(h_1, \xi)}{T'_n(h_1, \xi_1)} \right] \quad (7)$$

and

$$V_n(h_1, \eta) = \sqrt{1 - \eta^2} S_{1,n}^{(1)}(h_1, \eta) \quad (8)$$

$$U_n(h_1, \xi) = \sqrt{\xi^2 - 1} R_{1,n}^{(4)}(h_1, \xi) \quad (9)$$

$$T_n(h_1, \xi) = \sqrt{\xi^2 - 1} R_{1,n}^{(3)}(h_1, \xi) \quad (10)$$

where $S_{1,n}^{(1)}$ are the prolate spheroidal angular functions, $R_{1,n}^{(3)}$ and $R_{1,n}^{(4)}$ are the prolate spheroidal radial functions of third kind and fourth kind respectively [21], and $h_1 = 2\pi f d \sqrt{\epsilon_{r1} \mu_{r1} \epsilon_0 \mu_0} / 2$. In the case of an infinitesimally thin excitation slot, p_n can be expressed as

$$p_n \approx \frac{jw\epsilon_1 d}{2N_{1,n}(h_1)} \bar{V} V_n(h_1, \eta_0) \tag{11}$$

where \bar{V} is the applied voltage across the slot.

In region II ($\xi_2 \leq \xi \leq \xi_3$) and III ($\xi \geq \xi_3$), the auxiliary scalar wave functions A_2 and A_3 are given by

$$A_2 = \sum_{n=1,2}^{\infty} [M_n^2 U_n(h_2, \xi) + N_n^2 T_n(h_2, \xi)] V_n(h_2, \eta) \tag{12}$$

$$A_3 = \sum_{n=1,2}^{\infty} M_n^3 U_n(h_3, \xi) V_n(h_3, \eta) \tag{13}$$

where M_n^2 , N_n^2 and M_n^3 are the unknown expansion coefficients to be solved by boundary conditions, with $h_2 = 2\pi f d \sqrt{\epsilon_{r2} \mu_{r2} \epsilon_0 \mu_0} / 2$ and $h_3 = 2\pi f d \sqrt{\epsilon_{r3} \mu_{r3} \epsilon_0 \mu_0} / 2$.

To determine the unknown expansion coefficients, imposing the boundary conditions at spheroidal surfaces $\xi = \xi_2$ and $\xi = \xi_3$ which require the continuity of the tangential fields,

$$A_1 = A_2 \Big|_{\xi=\xi_2} \tag{14a}$$

$$\frac{1}{\epsilon_1} \frac{\partial A_1}{\partial \xi} = \frac{1}{\epsilon_2} \frac{\partial A_2}{\partial \xi} \Big|_{\xi=\xi_2} \tag{14b}$$

$$A_2 = A_3 \Big|_{\xi=\xi_3} \tag{14c}$$

$$\frac{1}{\epsilon_2} \frac{\partial A_2}{\partial \xi} = \frac{1}{\epsilon_3} \frac{\partial A_3}{\partial \xi} \Big|_{\xi=\xi_3} \tag{14d}$$

To solve these equations, the expansion form of V_n is used,

$$V_n(h, \eta) = \sum_{r=0,1}^{\infty} \sqrt{1 - \eta^2} d_r^{1,n}(h) P_{1+r}^1(\eta) \tag{15}$$

where $d_r^{1,n}(h)$ are the expansion coefficients which are nonzero when r is even (odd) and n is odd (even). And $P_{1+r}^1(\eta)$ is the associated

Legendre function. Comparing the coefficients of $P_{1+r}^1(\eta)$ in both sides of the equations, we can obtain a set of linear equations as follows,

$$\begin{bmatrix} [A] & -[C] & -[D] & \mathbf{0} \\ [E] & -[G] & -[H] & \mathbf{0} \\ \mathbf{0} & [J] & [K] & -[L] \\ \mathbf{0} & [O] & [P] & -[Q] \end{bmatrix} \begin{bmatrix} [M_n^1] \\ [M_n^2] \\ [N_n^2] \\ [M_n^3] \end{bmatrix} = \begin{bmatrix} -[B] \\ -[F] \\ \mathbf{0} \\ \mathbf{0} \end{bmatrix} \quad (16)$$

where the intermediate terms $A - Q$ are given in [26] and $\mathbf{0}$ is the zero matrix.

Once the expansion coefficients are solved, the EM fields of this antenna system would be known. In the far-field zone ($\xi \rightarrow \infty$), the magnetic and electric fields can be obtained as follows,

$$H_\phi \approx \frac{2e^{-jk_3r}}{k_3rd \sin \theta} \sum_{n=1,2}^{\infty} e^{j(\frac{n+1}{2})\pi} M_n^3 V_n(h_3, \cos \theta) \quad (17)$$

$$E_\theta \approx \sqrt{\frac{\mu_{r_3} \mu_0}{\epsilon_{r_3} \epsilon_0}} H_\phi \quad (18)$$

where $k_3 = \sqrt{\epsilon_{r_3} \mu_{r_3}} k_0$, and k_0 is the wavenumber in free space.

2.3. Radiation Power of Antenna-DNG System

The EM fields of prolate spheroidal antenna coated with DNG MTMs shell have been given in the last section. Therefore, the power radiated by antenna-DNG shell system can be obtained in terms of the integral of the Poynting vector over a closed surface containing the spheroidal antenna,

$$\begin{aligned} P_{\text{rad}} &= \frac{1}{2} \text{Re} \left[\iint_S (\mathbf{E} \times \mathbf{H}^*) \cdot \hat{\xi} dS \right] \\ &= \frac{1}{2} \text{Re} \left[\int_0^{2\pi} d\phi \int_{-1}^{+1} h_\phi h_\eta \left((-\hat{\eta}) E_\eta \times \hat{\phi} H_\phi^* \right) \cdot \hat{\xi} d\eta \right] \\ &= \pi \text{Re} \left[\int_{-1}^{+1} h_\phi h_\eta E_\eta H_\phi^* d\eta \right] \end{aligned} \quad (19)$$

where S is the surface of the confocal spheroid $\xi = \xi_3$. Substituting (4), (6) and (13) into (19), we obtain,

$$\begin{aligned} P_{\text{rad}} &= \text{Re} \left[\frac{j2\pi}{w\epsilon_3 d} \int_{-1}^{+1} (1 - \eta^2)^{-1} \frac{\partial A_3}{\partial \xi} A_3^* d\eta \right] \\ &= \text{Re} \left[\frac{j2\pi}{w\epsilon_3 d} \int_{-1}^{+1} (1 - \eta^2)^{-1} \left[\sum_{n=1,2}^{\infty} M_n^3 U_n'(h_3, \xi_3) V_n(h_3, \eta) \right] \right. \\ &\quad \left. \times \left[\sum_{n'=1,2}^{\infty} M_{n'}^3 U_{n'}'(h_3, \xi_3) V_{n'}(h_3, \eta) \right]^* \right] \end{aligned} \quad (20)$$

Using the orthogonality property of function $V_n(h, \eta)$,

$$\int_{-1}^1 (1 - \eta^2)^{-1} V_n(h, \eta) V_{n'}(h, \eta) d\eta = \begin{cases} N_{1,n}(h) & \text{if } n = n', \\ 0 & \text{if } n \neq n'. \end{cases} \quad (21)$$

The radiated power is obtained,

$$P_{\text{rad}} = \text{Re} \left[\frac{j2\pi}{w\epsilon_3 d} \sum_{n=1,2}^{\infty} |M_n^3|^2 U_n'(h_3, \xi_3) U_n^*(h_3, \xi_3) N_{1,n}(h_3) \right] \quad (22)$$

The current distribution on the spheroidal surface in the η direction can be expressed as

$$I(\eta) = \int_0^{2\pi} J_\eta h_\phi d\phi = \int_0^{2\pi} H_\phi|_{\xi=\xi_1} h_\phi d\phi = 2\pi A_1|_{\xi=\xi_1} \quad (23)$$

where J_η is the surface current, which is equal to $H_\phi|_{\xi=\xi_1}$ in magnitude. The ‘‘average current’’ I_{av} over the length along the angular direction on the surface of spheroidal dipole is defined as

$$I_{\text{av}} = \frac{\int_{-1}^{+1} I(\eta) h_\eta d\eta}{\int_{-1}^{+1} h_\eta d\eta} \quad (24)$$

Therefore, the radiated power by antenna system with 1 A average current can be obtained,

$$P_{\text{norm}} = \frac{P_{\text{rad}}}{|I_{\text{av}}|^2} \quad (25)$$

Finally, the radiated power ratio (RPR) can be expressed as follows,

$$RPR = \frac{P_{\text{norm, DNG shell}}}{P_{\text{norm, uncoated}}} \quad (26)$$

3. RESULTS AND DISCUSSION

An electrically small antenna in free space is defined as $k_0 r_e \leq 0.5$ in [5]. The frequency of interest here, $f_0 = 300$ MHz, the free space wavelength $\lambda_0 = 1.0$ m, and the electrically small antenna should be inside the sphere with radius $r_e = 79.58$ mm. For electrically small antennas, we need only consider the dominant lowest order mode ($n = 1$) to calculate the RPRs using (26). Region I and Region III as shown in Fig. 1 are assumed to be free space, i.e., $\epsilon_{r_1} = \epsilon_{r_3} = \epsilon_{r_0}$ and $\mu_{r_1} = \mu_{r_3} = \mu_0$.

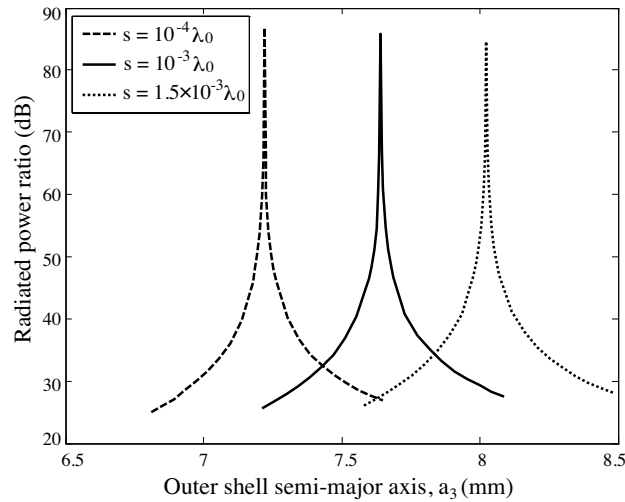


Figure 2. Radiated power of an infinitesimal electric dipole ($2a_1 = 10.0$ mm = $\lambda_0/100$, $\xi_1 = 1.005$) coated with a DNG shell ($\epsilon_{r_2} = -3.0$ and $\mu_{r_2} = -1.0$) for various thickness t (or a_3) at different separations s normalized by the power radiated by the same infinitesimal electric dipole in free space.

Figure 2 shows the RPRs of the infinitesimal electric dipole-DNG shell system versus the outer shell semi-major axis a_3 with different separations s between dipole and shell. The dipole antenna is modelled by thin spheroid ($\xi_1 = 1.005$, i.e., $a_1/b_1 = 10.0$). The total length of

antenna is $2a_1 = 10.0 \text{ mm} = \lambda_0/100$. It is shown that, with DNG shell ($\epsilon_{r_2} = -3.0$, $\mu_{r_2} = -1.0$), the infinitesimal electric dipole-DNG shell system has a natural resonance due to the cancellation of the inductive reactance introduced by DNG MTMs shell and the capacitive reactance of the electrically small antenna. It is seen that the maximum RPR is 85.78 dB at $a_{3,\max} = 7.64 \text{ mm}$ with $s = \lambda_0/1000$. It is found that the maximum RPR is enhanced by more than 20 dB comparing with the maximum RPR coated with the corresponding spherical ENG shell presented in [9] and the outer shell semi-major axis $a_{3,\max}$ is about 60% smaller than the corresponding radius of the outer ENG spherical shell ($r_{2,\max} = 18.79 \text{ mm}$). It is also seen that the peak of the RPR occurs at an increasing outer shell semi-major axis a_3 as the separation s increasing.

Figures 3(a) and (b) show the RPRs of the infinitesimal electric dipole-DNG shell system with different relative permittivity ϵ_{r_2} and different relative permeability μ_{r_2} of DNG shells respectively. It is found that a_3 of the peak of the RPR is approximately inverse proportional to the relative permittivity ϵ_{r_2} . However, the change of μ_{r_2} have no effect on the peak of the RPR. This is because only ϵ_{r_2} will change the effective reactance and this relation can be expressed as follows [9],

$$X_{\text{shell}} \propto jw_0 \frac{1}{w_0^2 |\epsilon_{r_2}| \Delta r} \quad (27)$$

where Δr is the thickness of the shell and in our case $\Delta r = t = b_3 - b_2$.

Figure 4 shows frequency dependence of the RPRs of the infinitesimal electric dipole-DNG shell system which is the same as the one considered in Fig. 2 with $a_3 = a_{3,\max} = 7.64 \text{ mm}$. Therefore, the FBW can be obtained by the relation [1, 8],

$$\text{FBW} = \frac{\Delta f_{3\text{dB}}}{f_{0\text{dB}}} = \frac{1}{Q_{\text{BW}}} \quad (28)$$

where $\Delta f_{3\text{dB}} = f_{+,3\text{dB}} - f_{-,3\text{dB}}$ and Q_{BW} is the radiation quality factor. $f_{+,3\text{dB}}$ and $f_{-,3\text{dB}}$ denote the frequencies above and below $f_{0\text{dB}}$ where the RPR is 3 dB lower than its maximum value. It is found that, in Fig. 4, the maximum value of RPR is 86.45 dB at $f_{0\text{dB}} = 297.19 \text{ MHz}$, $f_{-,3\text{dB}} = 290.21 \text{ MHz}$ and $f_{+,3\text{dB}} = 304.01 \text{ MHz}$. Therefore, the $\text{FBW}_{\text{DNG}} = 4.64\%$ and the quality factor $Q_{\text{BW,DNG}} = 21.55$.

Figure 5 shows the RPRs of an electrically small dipole ($2a_1 = 20.0 \text{ mm} = \lambda_0/50$) coated with a DNG shell. It is found that, at

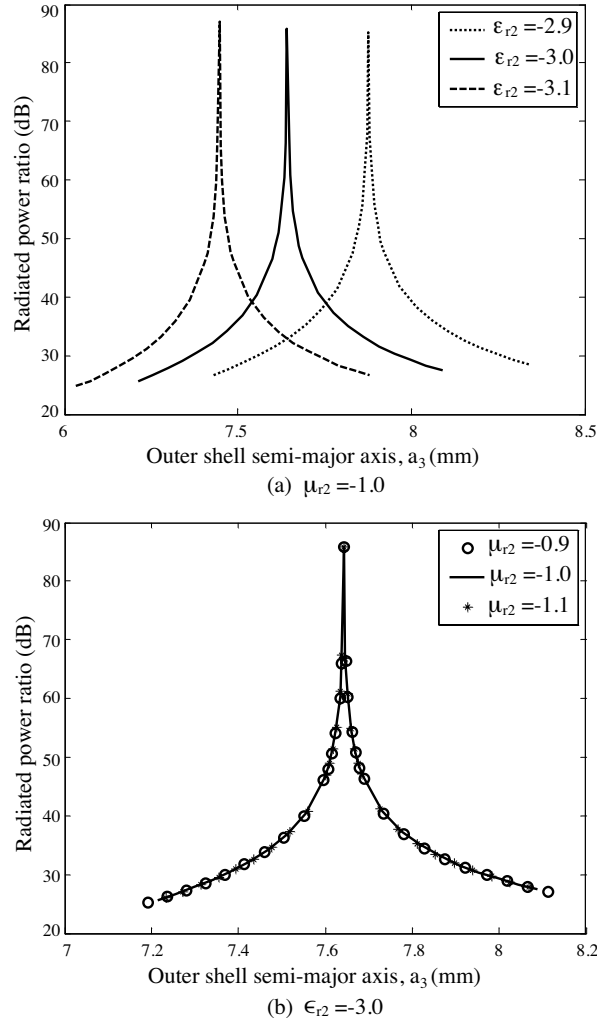


Figure 3. Radiated power of an infinitesimal electric dipole ($2a_1 = 10.0$ mm = $\lambda_0/100$, $\xi_1 = 1.005$) coated with DNG shells, (a) $\mu_{r2} = -1.0$ and different ϵ_{r2} , (b) $\epsilon_{r2} = -3.0$ and different μ_{r2} , at separation $s = \lambda_0/1000$ normalized by the power radiated by the same infinitesimal electric dipole in free space.

$a_{3,\max} = 14.78$ mm, the maximum RPR is 68.85 dB which is 16.93 dB smaller than the one with $2a_1 = \lambda_0/100$ presented in Fig. 2. This is because the size of this dipole-DNG antenna system is 43% larger than

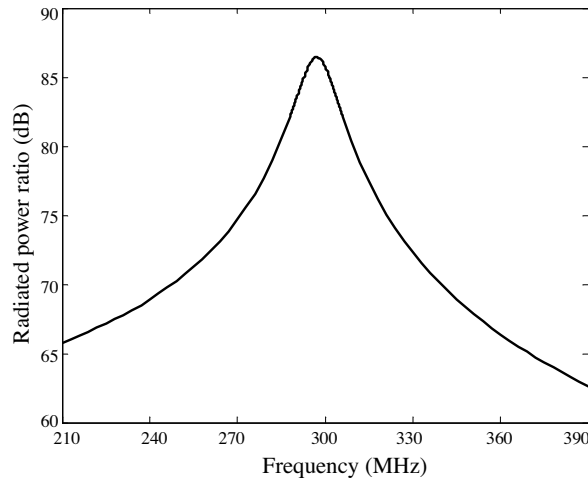


Figure 4. Frequency dependence of radiated power of an infinitesimal electric dipole ($2a_1 = 10.0 \text{ mm} = \lambda_0/100$, $\xi_1 = 1.005$) coated with a DNG shell ($\epsilon_{r_2} = -3.0$ and $\mu_{r_2} = -1.0$) at separation $s = \lambda_0/1000$ with $a_3 = 7.64 \text{ mm}$ normalized by the power radiated by the same infinitesimal electric dipole in free space.

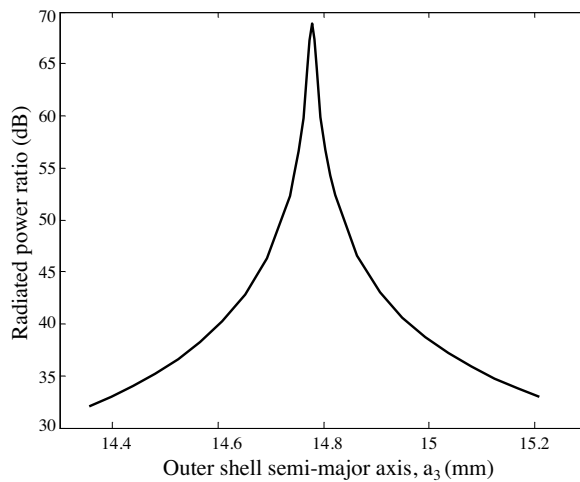


Figure 5. Radiated power of an electrically small dipole ($2a_1 = 20.0 \text{ mm} = \lambda_0/50$, $\xi_1 = 1.005$) coated with a DNG shell ($\epsilon_{r_2} = -3.0$ and $\mu_{r_2} = -1.0$) at separation $s = \lambda_0/1000$ normalized by the power radiated by the same electrically small dipole in free space.

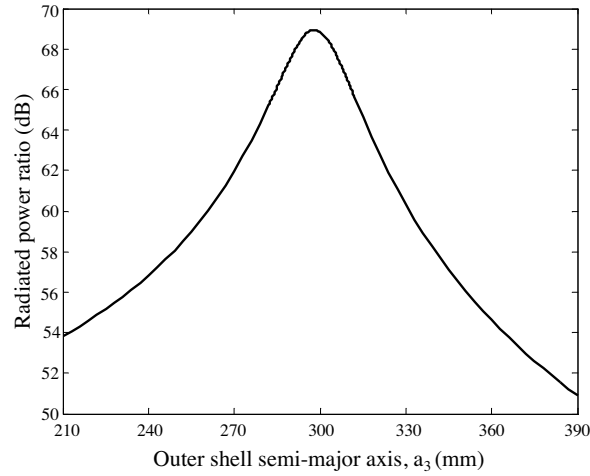


Figure 6. Frequency dependence of radiated power of an electrically small dipole ($2a_1 = 20.0 \text{ mm} = \lambda_0/50$, $\xi_1 = 1.005$) coated with a DNG shell ($\epsilon_{r_2} = -3.0$ and $\mu_{r_2} = -1.0$) at separation $s = \lambda_0/1000$ with $a_3 = 14.78 \text{ mm}$ normalized by the power radiated by the same electrically small dipole in free space.

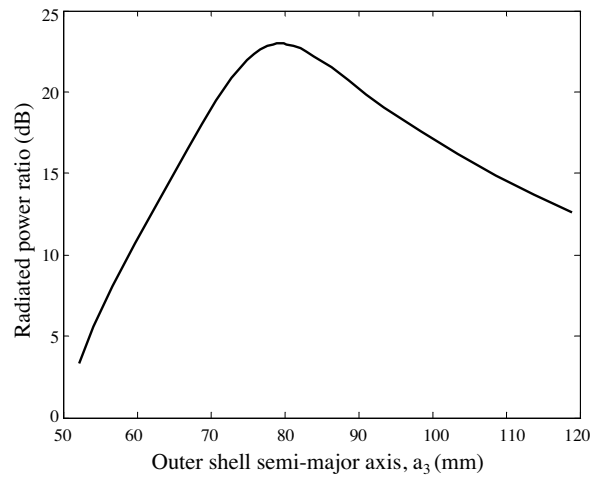


Figure 7. Radiated power of an electrically small dipole ($2a_1 = 100.0 \text{ mm} = \lambda_0/10$, $\xi_1 = 1.005$) coated with a DNG shell ($\epsilon_{r_2} = -3.0$ and $\mu_{r_2} = -1.0$) at separation $s = \lambda_0/1000$ normalized by the power radiated by the same electrically small dipole in free space.

that considered in Fig. 2.

In Fig. 6, it is found that the maximum value of RPR is 68.94 dB at $f_{0\text{dB}} = 298.07$ MHz, $f_{-,3\text{dB}} = 284.39$ MHz and $f_{+,3\text{dB}} = 311.15$ MHz. Therefore, the $\text{FBW}_{\text{DNG}} = 8.98\%$ and the quality factor $Q_{\text{BW, DNG}} = 11.14$. From above figures, it is found that, with the increasing size of antenna system, the maximum value of RPR and the quality factor Q decrease, while the FBW increases.

Figure 7 shows the RPRs of an electrically small dipole ($2a_1 = 100.0$ mm = $\lambda_0/10$) coated with a DNG shell. It is found that the maximum RPR is 22.98 dB at $a_{3,\text{max}} = 79.39$ mm which is just a little bit smaller than the maximum radius of the electrically small antenna 79.58 mm at 300 MHz. It can be seen that the peak value of RPR of this electrically small dipole-DNG system is reduced more than 60 dB comparing with the one with $2a_1 = \lambda_0/100$ presented in Fig. 2 due to the larger size of antenna.

4. CONCLUSION

An efficient, electrically small prolate spheroidal antenna coated with confocal DNG MTMs shell is presented in this paper. Using the method of separation of the spheroidal scalar wave functions, the radiation power of this antenna-DNG shell system excited by a delta voltage across an infinitesimally narrow gap around the antenna center is obtained. It is found that this electrically small dipole-DNG shell system has very high radiation efficiency comparing with the normal electrically small antenna. It is found that the spheroidal shell can achieve more compact structure and higher radiated power ratio than the corresponding spherical shell. This dipole-DNG shell systems with different sizes (up to $\lambda/10$) are analyzed and discussed. It is found that the maximum value of RPR and the quality factor Q decrease due to the size of antenna system increasing, while the FBW of this electrically small dipole-DNG shell system increases with antenna size increasing.

REFERENCES

1. Balanis, C. A., *Antenna Theory: Analysis and Design*, John Wiley & Sons, New York, 2005.
2. Chu, L. J., "Physical limitations of omnidirectional antennas," *J. Appl. Phys.*, Vol. 19, No. 12, 1163–1175, 1948.
3. Hansen, R. C., "Fundamental limitations in antennas," *Proc. IEEE*, Vol. 69, No. 2, 170–181, 1981.

4. McLean, J. S., "A re-examination of the fundamental limits on the radiation Q of electrically small antennas," *IEEE Trans. Antennas Propag.*, Vol. 44, No. 5, 672–676, 1996.
5. Best, S. R., "A discussion on the properties of electrically small self-resonant wire antennas," *IEEE Antennas Propag. Mag.*, Vol. 46, No. 6, 9–22, 2004.
6. Kyi, Y. and J.-Y. Li, "Analysis of electrically small size conical antennas," *Progress In Electromagnetics Research Letters*, Vol. 1, 85–92, 2008.
7. Engheta, N. and R. W. Ziolkowski, "A positive future for double-negative metamaterials," *IEEE Trans. Antennas Propag.*, Vol. 53, No. 4, 1535–1556, 2005.
8. Ziolkowski, R. W. and A. D. Kipple, "Application of double negative materials to increase the power radiated by electrically small antennas," *IEEE Trans. Antennas Propag.*, Vol. 51, No. 10, 2626–2640, 2003.
9. Ziolkowski, R. W. and A. Erentok, "Metamaterials-based efficient electrically small antennas," *IEEE Trans. Antennas Propag.*, Vol. 54, No. 7, 2113–2130, 2006.
10. Grzegorzczuk, T. M. and J. A. Kong, "Review of left-handed metamaterials: Evolution from theoretical and numerical studies to potential applications," *J. Electromagn. Waves Appl.*, Vol. 20, No. 14, 2053–2064, 2006.
11. Chen, H., B.-I. Wu, and J. A. Kong, "Review of electromagnetic theory in left-handed materials," *J. Electromagn. Waves Appl.*, Vol. 20, No. 15, 2137–2151, 2006.
12. Wang, M. Y., J. Xu, J. Wu, Y. Yan, and H.-L. Li, "FDTD study on scattering of metallic column covered by double-negative metamaterial," *J. Electromagn. Waves Appl.*, Vol. 21, No. 14, 1905–1914, 2007.
13. Manzanares-Martinez, J. and J. Gaspar-Armenta, "Direct integration of the constitutive relations for modeling dispersive metamaterials using the finite difference time-domain technique," *J. Electromagn. Waves Appl.*, Vol. 21, No. 15, 2297–2310, 2007.
14. Yang, R., Y.-J. Xie, D. Li, J. Zhang, and J. Jiang, "Bandwidth enhancement of microstrip antennas with metamaterial bilayered substrates," *J. Electromagn. Waves Appl.*, Vol. 21, No. 15, 2321–2330, 2007.
15. Hamid, A.-K. and F. R. Cooray, "Radiation characteristics of a spheroidal slot antenna coated with isorefractive materials," *J. Electromagn. Waves Appl.*, Vol. 21, No. 12, 1605–1619, 2007.

16. Zainud-Deen, S. H., A. Z. Botros, and M. S. Ibrahim, "Scattering from bodies coated with metamaterial using FDFD method," *Progress In Electromagnetics Research B*, Vol. 2, 279–290, 2008.
17. Valagiannopoulos, C. A., "Electromagnetic scattering from two eccentric metamaterial cylinders with frequency-dependent permittivities differing slightly each other," *Progress In Electromagnetics Research B*, Vol. 3, 23–34, 2008.
18. Hady, L. K. and A. A. Kishk, "Electromagnetic scattering from conducting circular cylinder coated by meta-materials and loaded with helical strips under oblique incidence," *Progress In Electromagnetics Research B*, Vol. 3, 189–206, 2008.
19. Cui, T. J., H.-F. Ma, R. P. Liu, B. Zhao, Q. Cheng, and J. Y. Chin, "A symmetrical circuit model describing all kinds of circuit metamaterials," *Progress In Electromagnetics Research B*, Vol. 5, 63–76, 2008.
20. Lagarkov, A. N., V. N. Kisel, and V. N. Semenenko, "Wide-angle absorption by the use of a metamaterial plate," *Progress In Electromagnetics Research Letters*, Vol. 1, 35–44, 2008.
21. Flammer, C., *Spheroidal Wave Functions*, Stanford University Press, Stanford, 1957.
22. Cooray, M. F. R. and I. R. Ciric, "Scattering of electromagnetic waves by a coated dielectric spheroid," *Journal of Electromagnetic Waves and Applications*, Vol. 6, 1491–1507, 1992.
23. Huang, M. D. and S. Y. Tan, "Spheroidal phase mode processing for antenna arrays," *Journal of Electromagnetic Waves and Applications*, Vol. 19, No. 11, 1431–1442, 2005.
24. Schelkunoff, S. A., *Advanced Antenna Theory*, Wiley, New York, 1952.
25. Do-Nhat, T. and R. H. MacPhie, "The input admittance of thin prolate spheroidal dipole antennas with finite gap widths," *IEEE Trans. Antennas Propag.*, Vol. 43, No. 11, 1243–1252, 1995.
26. Li, L. W., M. S. Leong, T. S. Yeo, and Y. B. Gan, "Electromagnetic radiation from a prolate spheroidal antenna enclosed in a confocal spheroidal radome," *IEEE Trans. Antennas Propag.*, Vol. 50, No. 11, 1525–1533, 2002.
27. Capoglu, I. R. and G. S. Smith, "The input admittance of a prolate-spheroidal monopole antenna fed by a magnetic frill," *IEEE Trans. Antennas Propag.*, Vol. 54, No. 2, 572–585, 2006.